Bioconjugate Chemistry

Review

pubs.acs.org/bc

Multifunctional Ultrasound Contrast Agents for Imaging Guided Photothermal Therapy

Caixin Guo,[†] Yushen Jin,[†,‡] and Zhifei Dai*[,‡]

[†]School of Life Science and Technology, Harbin Institute of Technology, Harbin 150080, China

[‡]Department of Biomedical Engineering, College of Engineering, Peking University, Beijing 100871, China

ABSTRACT: Among all the imaging techniques, ultrasound imaging has a unique advantage due to its features of real-time, low cost, high safety, and portability. Ultrasound contrast agents (UCAs) have been widely used to enhance ultrasonic signals. One of the most exciting features of UCAs for use in biomedicine is the possibility of easily putting new combinations of functional molecules into microbubbles (MBs), which are the most routinely used UCAs. Various therapeutic agents and medical nanoparticles (quantum dots, gold, Fe_3O_4, etc.) can be loaded into ultrasound-responsive MBs. Hence, UCAs can be developed as multifunctional agents that integrate capabilities for early detection and diagnosis and for imaging guided therapy of various diseases. The current review will focus on such state-of-the-art UCA platforms that have been exploited for multimodal imaging and for imaging guided photothermal therapy.

INTRODUCTION

Currently, several imaging modalities have rapidly advanced, such as ultrasound (US) imaging, magnetic resonance imaging (MRI), and computer tomography (CT).[1−4] With the use of related contrast agents, the sensitivity and resolution of clinical imaging have experienced great improvements. Nevertheless, each imaging modality has its own advantages and intrinsic limitations, and thus, modality selection for clinical diagnostic imaging is a challenge. The imaging modalities with high resolution have relatively poor sensitivity, while those with high sensitivity have relatively poor resolution. Among all the imaging techniques, US imaging has the unique advantages of being a real-time technique with low cost, high safety, and ready availability via portable devices. However, many cancers cannot be detected via US imaging. Calcifications that are visible on mammograms cannot be detected by ultrasound scans, preventing the early diagnosis of the breast cancers that begin with calcifications. CT is one of the most routinely applied medical systems with high spatial resolution, unlimited penetration depth, and facility to 3-D visual reconstruction of tissues of interest. However, the inherently low sensitivity of CT imaging induces poor soft tissue contrast, and repeated CT scans deliver a relatively high dose of radiation to the patient. MRI is also noninvasive and can offer exquisite soft tissue contrast and multiplanar images, but it is low sensitivity, high cost, and cannot provide real-time images with its relatively long processing time.

The idea of using multiple modalities in conjunction with one another has recently gained popularity. The first fused positron emission tomography (PET)/CT instrument was commercially available in 2001. In addition, the emergence of the fused PET/MRI instrument expands imaging frontiers. The ACUSON S3000 ultrasound system from Siemens enables the automatic fusion of ultrasound with 3-D CT volumes. The complementary capabilities of different imaging modalities can be harnessed to great effect by using these instruments in tandem. These multimodal imaging instruments have attracted extensive interest in the design and development of multimodal contrast agents to boost the clinical benefits of hybrid instrument technology. Multimodal imaging agents, which permit the combination of two or more imaging modalities by using a single agent, can provide multimodal contrast imaging concurrently with complementary temporal, spatial, and depth resolution for more accurate and reliable diagnosis. In view of the intrinsic limitations of US, the integration of US with other imaging modalities into a single agent will compensate for the deficiencies of US imaging and maximize the advantages of each imaging modality.

"Theranostics", a term derived from thera(py) plus (diag)-nostics to connect the fields of diagnostics and therapeutics, is hoped to improve patient treatment effects and safety through more personalized therapies for various diseases. More efforts have recently been concentrated on integrating imaging probes and therapeutic species into a single agent for concurrent disease detection and targeted drug delivery or imaging-guided drug delivery. Various imaging technologies, such as US, optical imaging, MRI, and CT, can be used for theranostics. Theranostic agents can deliver small molecules, biologics (such as proteins and siRNA) or nanoparticles (NPs) to

Received: March 6, 2014
Revised: April 29, 2014
Published: April 29, 2014

   dx.doi.org/10.1021/bc500092h | *Bioconjugate Chem.* 2014, 25, 840−854

disease targets in an attempt to achieve targeted therapy or imaging-guided therapy.

UCAs have been widely used to enhance ultrasonic signals. The most routinely used UCAs can be prepared as aqueous dispersions of water-insoluble gas (e.g., perfluorocarbon) MBs coated with a thin shell made of proteins,[5] polymers,[6,7] lipids,[8,9] or surfactants.[10,11] One of the most exciting features of UCAs for use in biomedicine is the possibility of loading multiple functional components, such as several therapeutic species and/or medical NPs (drugs, genes, quantum dots (QDs), gold, and Fe_3O_4, etc.), into the shell and core domain of ultrasound-responsive MBs to enable their application of multiple purposes, e.g., diagnosis and therapy, or multimodal imaging, as indicated in Figure 1. The combination of multiple functionalities in the same agent can prevent the additional pressure on the body's blood clearance mechanisms that can accompany the administration of multiple doses of agents. Therefore, ultrasonically active MBs possess a natural superiority for accomplishing simultaneous imaging and therapy.

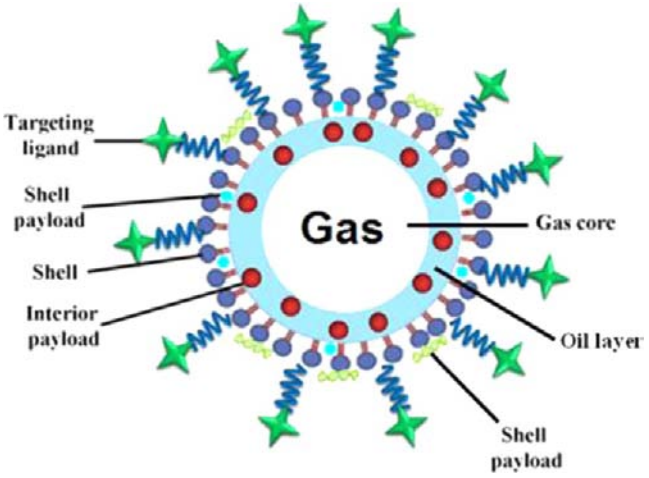

Figure 1. Multifunctional ultrasound contrast agent constructed by loading multiple functional components into the shell and core domain of MBs.

Photothermal therapy as a minimally invasive alternative to conventional surgical treatment has been widely used for tumor ablation treatment because of its accurate energy delivery to target tissue and because of the sensitivity of tumor tissue to temperature increases.[12,13] Light in the near-infrared region (NIR) in combination with appropriate light-absorbing agents is especially attractive for selective photothermal interaction due to the low absorbance of human tissues in this region.[14] The combination of US imaging and photothermal therapy by loading various NIR-absorbing species into UCAs has attracted more and more attention. US imaging has identified the location and size of tumors, and NIR laser and photoabsorbers were subsequently used to ablate tumors by site-specific photothermal therapy with no damage to the normal tissue. In the current review, we will focus on the state-of-the-art UCA platforms that have been exploited for multimodal imaging and imaging-guided photothermal therapy. The expectation of this article is to stimulate broad research interest in this promising emerging field.

PREPARATION APPROACHES FOR ULTRASOUND-BASED MULTIFUNCTIONAL AGENTS

Polymer/lipid/surfactant-shelled and gas-filled MBs can be prepared by several methods, such as sonication,[15−17] high shear emulsification,[18,19] membrane emulsification,[20] inkjet printing,[21] electrohydrodynamic atomization,[22,23] and microfluidic processing.[24,25] Novel MBs with high stability were recently prepared by ultrasonicating a mixture of poly(ethylene glycol) 40 stearate (PEG40S) and Span 60 surfactants,[26] and the preparation of novel MBs is illustrated in Figure 2. MBs composed of polymers, especially poly(lactic acid) (PLA) or poly(lactide-*co*-glycolide acid) (PLGA), with excellent biocompatibility and biodegradability show good ultrasound contrast-enhanced abilities and other advantages: the good mechanical strength makes them stable; either hydrophobic or hydrophilic species or both can be loaded in them during the double emulsion fabrication procedure to become functionalized; and the charged surface and functional groups on the surface make easily modified to enable more uses such as site-targeted capabilities.[27] The water-in-oil-in-water (W/O/W) double emulsion method was generally employed to generate such polymeric MBs from PLA and poly(vinyl alcohol) (PVA) materials (Figure 3).[28] Ultrasonically active MBs are of particular interest because of their potential for entrapping

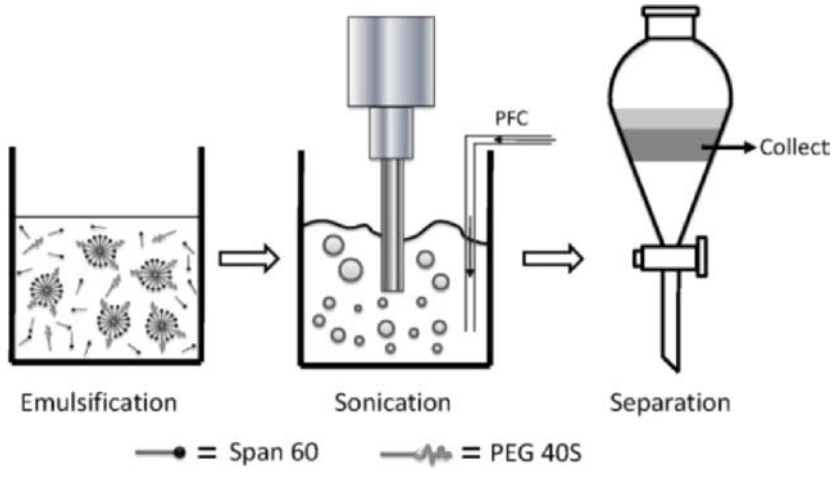

Figure 2. Schematic illustration of the formation of MBs using Span 60 and PEG40S. Reprinted with permission from ref 26.

dx.doi.org/10.1021/bc500092h | *Bioconjugate Chem.* 2014, 25, 840−854

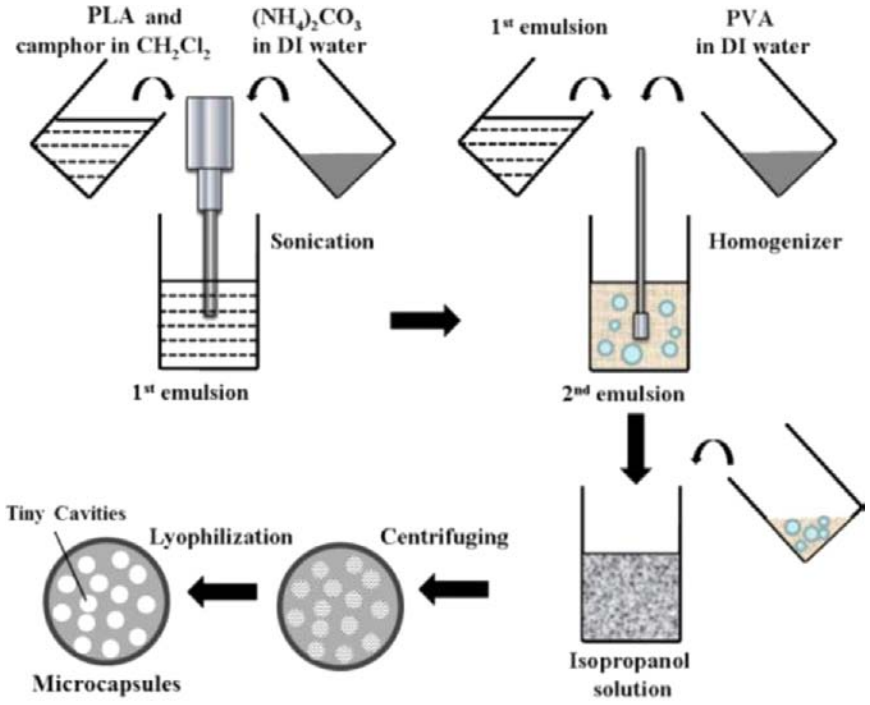

Figure 3. Schematic illustration of the formation of PLA MBs by water-in-oil-in-water double emulsion method, the picture was obtained from the ref 28 with a slight modification.

various functional molecules and therapeutic agents inside their shells or within their empty core domains. Therefore, it is very easy to add new combinations of molecules and thus new functionalities into such MBs to create smart UCAs. Next, we will focus on the drug loading method and coupling chemistry of other diagnostic or therapeutic agents with ultrasound MBs.

Drugs or other functional nanoparticles can generally be loaded into MBs through two methods, namely, the surface loading of performed MBs and entire volume loading. The loading approach was determined by the shell composition as well as the drug's physicochemical properties, such as its solubility, electrostatic charge, and particle size. For instance, electrostatically charged phospholipids can be used to bind oppositely charged drugs. Smaller species, such as QDs, superparamagnetic iron oxide (SPIO), and functional molecules, can be conjugated to the shell surface or encapsulated into the interior of the MBs without having a significant impact on the MB stability. However, larger nanoparticles, such as nanorods and nanoshells, may induce the disruption of MBs from phospholipids, proteins, or surfactants when loading these larger NPs onto the shell of the performed MBs. Nevertheless, the polymeric shelled MBs have the advantage of loading larger NPs because of their higher stability. Both hydrophobic and hydrophilic species can be encapsulated into polymeric shelled MBs;[29] however, the loading amount of hydrophilic drugs is smaller than that of lipophilic drugs because the aqueous phase comprises only a small portion of the MB volume. Protein, especially human serum albumin (HSA), has a high affinity for DNA and a large quantity of drug molecules. Drug loading can be performed during the production of MB by incubating the proteins with the drugs. Furthermore, HSA has abundant thiol groups, can form stable covalent bridges[30] by using a probe-type sonication method, and is therefore most widely used as an MB shell protein.

Magnetic NPs can be coupled to the shell surface of the MBs, embedded in the shells or the oil layer of the MBs by means of electrostatic interaction, hydrophobic interactions, or merely by physical encapsulation. Soetanto et al.[31] linked positively charged magnetite particles and negatively charged surfactant MBs by electrostatic interaction. Yang et al.[32] used a double-emulsion procedure to embed SPIO NPs into the oil layer of the polymer MBs. Chow et al.[33] and Liu et al.[34] synthesized magnetic MBs by encapsulating iron oxide NPs into the MB shells. In addition, Brismar et al.[35] covalently tethered SPIO NPs onto the surface of PVA MBs in which the SPIO NPs were functionalized via silanization to introduce amino groups, which then reacted with the aldehyde groups of PVA MBs through reductive amination. US/fluorescent dual-modal imaging agents can be prepared by conjugating fluorescent agents and MBs. For example, Ke et al.[36] electrostatically deposited fluorescent CdTe QDs onto the surface of surfactant MBs by using a layer-by-layer assembly technique. Indocyanine green (ICG), a water-soluble fluorescent imaging agent, was loaded into PLGA MBs by physical encapsulation.[37] HSA was attached to gold nanorods (GNRs) through free thiol groups in HSA, and the subsequent sonication of gold nanorods-HSA solution resulted in the formation of Au MBs, which presented an imaging ability with ultrasound/photoacoustic dual-modality.[38] To achieve simultaneous diagnosis and therapy, the near-infrared photo-absorber GNRs were adsorbed onto the surface of PLA microcapsules via electrostatic interaction.[39] Alternatively, imaging or therapeutic agents can be associated with smaller particles, which are in turn attached to the MBs. For example, CdSe/ZnS QDs, Au NRs, Fe_3O_4 NPs and Gd-loaded mesoporous silica NPs were incorporated into MBs via electrostatic interactions.[40] The surface charge of MBs as stabilized by lysozymes can be regulated by changing the pH value to attach negatively charged silica-coated NPs. The use of silica NPs as a secondary carrier to encapsulate various imaging

dx.doi.org/10.1021/bc500092h | *Bioconjugate Chem.* 2014, 25, 840−854

and therapeutic agents is independent of the agent sizes, shapes, and materials, and it shows great potential for preparing multifunctional UCAs by simple attachment.

In summary, it is difficult to say what is the best way to prepare multifunctional MBs with excellent stability, high targeting, monodispersivity, imaging, or theranostic capacities. Personal preparation approaches should be employed on the basis of the different properties of multifunctional agents and the corresponding requirements. Additionally, the processing cost will have to be considered, and therefore, the development of novel preparation methods is still a challenge for future research.

■ ULTRASOUND-BASED MULTIFUNCTIONAL IMAGING AGENTS

As mentioned above, each imaging modality has its own advantages and intrinsic limitations, and individual imaging modality only reveals a small piece of a complex confusion in disease etiology. Encapsulating multiple imaging agents in UCAs opens a new avenue for the simultaneous acquisition of anatomical, functional, and molecular information about biological tissue.[41−43] Multifunctional imaging modalities based on MRI, optical, PET, and CT have been well documented,[44] but US-based multifunctional imaging agents are still in their infancy.

US/MR Dual-Modal Imaging Agents. The best-established US-based multimodal imaging technology is a combination of US imaging and MRI. As mentioned above, although US imaging is a real-time and noninvasive imaging technique, its signal is usually disturbed by many factors. The ability of ultrasound to display tissue structure is worse than that of MRI. Moreover, the different physical compositions of US and MR contrast agents have resulted in different tracer distributions within the vasculature. US microbubble contrast agents are primarily intravascular,[45,46] whereas typical MRI contrast agents such as Gd-DTPA or SPIO NPs are capable of extravasation because of their low molecular weight or small size.[47,48] Thus, the integration of the two contrast agents can provide signals from the blood pool and surrounding tissue simultaneously. Ao et al.[49] reported the feasibility of Gd-DTPA-loaded PLGA MBs as both a US and MRI contrast agent. Gu et al.[32,50,51] and Liu et al.[34] developed a US-MRI dual-modal contrast agent by incorporating SPIO NPs into the shell of PLA and poly(butyl cyanoacrylate) MBs. The SPIO-PLA MBs are represented schematically in Figure 4. *In vitro* and *in vivo* MRI experiments showed that both the SPIO NP-inclusion MBs provided enhanced contrast for the MRI. Moreover, the inclusion of SPIO NPs enhanced the echogenicity of the host MBs compared with the unmodified one.[32,50] When poly(butyl cyanoacrylate) MBs were destructed by US, a significant increase in the longitudinal and transversal relaxivities was observed, demonstrating their triggerable MRI properties.[34]

Multimodal functionality does not always require the incorporation of multiple molecular species because some molecules themselves can be detected by more than one modality. It is not only convenient to medical professionals but also reduces the production and health-care costs. Ultrasonically active gas-filled MBs were also detectable by MRI because the shell oscillations of bubbles resulted in a proportionate contribution to magnetic susceptibility;[52] the contrast is particularly evident when the core gas is paramagnetic.[53] Another good example of material with dual properties is perfluorocarbons, which are detectable by both US and MRI.

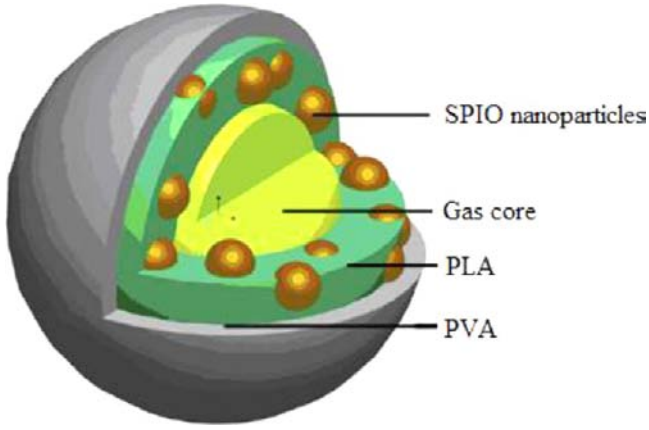

Figure 4. Schematic diagram of the SPIO NPs incorporated MBs generated by double emulsion method from PLA as the first shell containing SPIO NPs and PVA as the second shell. Reprinted with permission from ref 32.

Pisani et al.[54] reported that the perfluorooctyl bromide (PFOB) polymeric capsules can serve as US and MRI dual-model contrast agents. It is very interesting that the capsule diameter can be precisely tuned between 70 nm (nanocapsule) and 25 μm (microcapsule), which is consistent with imaging requirements, because the ideal agent size should be tailored to either limit circulation to the vascular space (micrometric but less than ~7 μm) or allow passage beyond the endothelium depending on the compartment of the biological target.

US/Optical Dual-Modal Imaging Agents. Optical imaging has high sensitivity and multicolor imaging capabilities, but its low spatial resolution in tissue from the strong scattering of both excitation and emission lights has blocked its wide application to clinical diagnosis in humans. Compared with fluorescence imaging, which is seriously limited for *in vivo* applications owing to the weak penetration depth of light, US has become an outstanding technique in clinical diagnosis because it is possible to obtain highly resolved 3D images of living bodies. Moreover, such a scattering artifact of the excitation source in optical imaging can be inhibited by ultrasound. As early as 2000, optical imaging was used as an effective adjunct to ultrasound in discriminating benign from malignant breast lesions, improving ultrasound specificity, and reducing unnecessary biopsies.[55] Therefore, the contrast agents that combine fluorescence and US imaging have received a great deal of attention because they integrate the high sensitivity of the fluorescence phenomenon with the high spatial resolution of US. Our group recently[36] reported a US-fluorescent dual-modal imaging agent through the layer-by-layer deposition of poly(allylamine hydrochloride) and CdTe QDs onto ST68 MBs (Figure 5). CdTe QDs-modified MBs not only presented significant ultrasound contrast enhancement in rabbit kidney and hypodermic fluorescent imaging in nude mice (Figure 6 and Figure 7), but also have the potential to deliver QDs to the disease site for cell and tissue fluorescent imaging by ultrasound targeted microbubble destruction (UTMD) technique.[56−59]

Seo et al.[40] also prepared multifunctional MBs by incorporating various silica-coated NPs, such as CdSe/ZnS QDs, gold nanorods, iron oxide NPs, and Gd-loaded NPs, onto monodisperse, protein−lipid-coated perfluorobutane MBs that were generated via microfluidics. Such NP-loaded MBs demonstrated the great prospects of US-optical, US-photo-

dx.doi.org/10.1021/bc500092h | *Bioconjugate Chem.* 2014, 25, 840−854

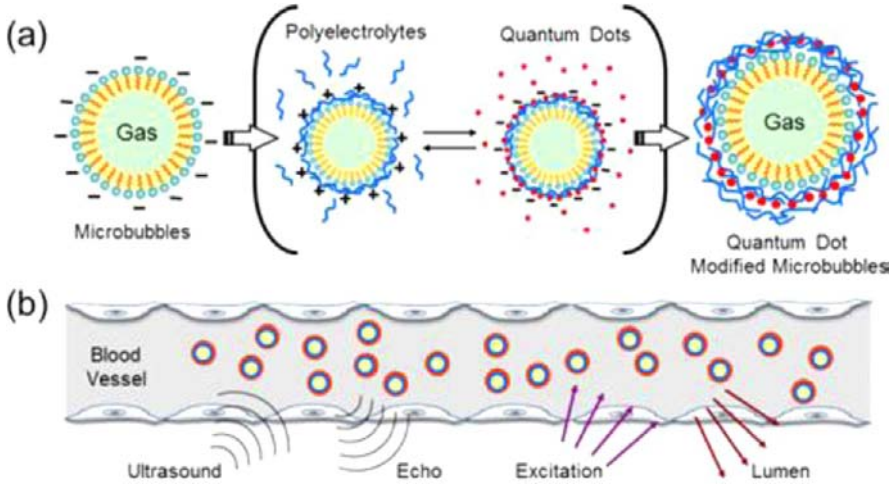

Figure 5. Schematic QDs-modified MBs: (a) fabrication process; (b) capability to serve as a dual-modal contrast agent for both US and optical imaging. Reprinted with permission from ref 36.

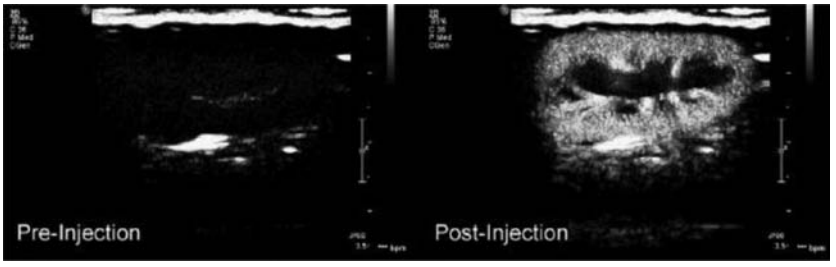

Figure 6. Pulse inversion harmonic images of the rabbit right kidney: (left) pre- and (right) postinjection of 0.1 mL kg^{-1} of QDs-modified MBs. Reprinted with permission from ref 36.

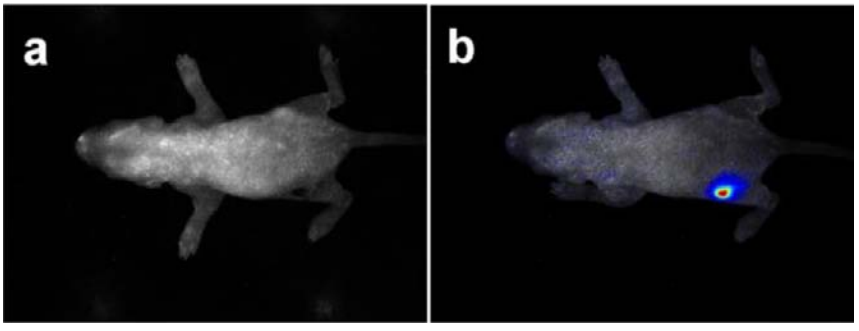

Figure 7. Photographs of mouse before (a) and after (b) injection of QDs-modified MBs.

acoustic (PA), US-MR dual-modal imaging, as well as US imaging-photothermal therapy applications.

ICG is one of the first optical contrast agents that was approved by the Food and Drug Administration for clinical imaging applications.[60−62] It is commonly used as a blood pool imaging agent because of its strong affinity to plasma proteins in the vascular system. As the fluorescence emission peak of ICG is located in the NIR region, the light can penetrate through thick biological tissues. Xu et al.[37] reported the use of ICG-encapsulated PLGA MBs for concurrent NIR and US imaging as illustrated in Figure 8, in which typical NIR fluorescence and B-mode US images were captured synchronously with the position and time. In addition to fluorescence imaging, ICG exhibited excellent photothermal,[63] photodynamic,[64] and photoacoustic[65] effects. Thus, it is technically feasible to demonstrate concurrent US, photoacoustic, and fluorescence imaging or US imaging-guided photothermal or photodynamic therapy, if encapsulating ICG in MBs.

US/Photoacoustic Imaging Agents. Despite the high sensitivity of pure optical imaging, this technique suffers from either shallow penetration depth or poor spatial resolution due to strong light scattering. Photoacoustic imaging integrates the spatial resolution of US imaging and the molecular sensitivity of optical imaging,[66] and it has emerged as a promising imaging technique for visualizing optically absorbing structures. When a pulsed laser is used to irradiate the subject, the laser pulse energy was absorbed by a chromophore, inducing local thermal expansion and producing a pressure transient. PA imaging is based on the use of the detected acoustic signals to reconstruct the optical absorption distribution. The functional properties of subcutaneous tissue structures in a cross-sectional area or a three-dimensional space can be detected by the PA effect.[67] A conventional US system can easily be combined with PA

dx.doi.org/10.1021/bc500092h | *Bioconjugate Chem.* 2014, 25, 840−854

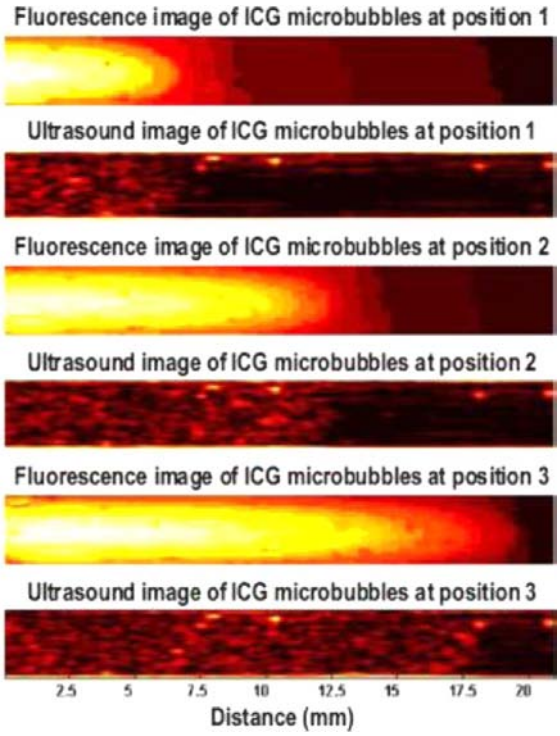

Figure 8. Typical ultrasound and fluorescence images of ICG-encapsulated MBs injected in a transparent tube. Reprinted with permission from ref 37.

imaging by encapsulating highly optical absorbing agents into MBs to provide both mechanical contrast (morphological information) and optical contrast (morphological and functional information). Moreover, it is feasible to integrate US and PA imaging into one imaging machine, thereby allowing the acquisition of both ultrasonic and PA imaging information during one imaging examination.

Gold nanoparticles are highly absorbing optical contrast agents that can be loaded in MBs and nanobubbles (NBs) for PA and US dual-modal imaging. Various gold NPs, such as nanospheres, nanocages, and nanorods, have been synthesized for enhancing photoacoustic imaging.[68−70] Gold nanosphere-loaded perfluorocarbon (PFC) droplets have been encased in bovine serum albumin to form photoacoustic nanodroplets, and simultaneous PA and US contrasts can be observed from polyacrylamide phantoms after embedding gold nanosphere-loaded PFC droplets.[71] The same group also prepared lipid PFC nanodroplets with encapsulated gold nanorods, which vaporized when exposed to pulsed laser irradiation, sending out a strong photoacoustic signal, and then formed into MBs that were detectable by ultrasound.[72]

Kim et al.[73] developed India ink-loaded PLGA MBs and NBs, which operated a novel dual-modality contrast agent for both US and PA imaging at different concentrations in gelatin phantoms (Figure 9). Moreover, the eight targets of ink-loaded PLGA bubbles are still visible even when chicken breast tissue of 18 mm thickness was added to the top of the gelatin phantom (Figure 10), indicating that one potential application for these PLGA bubbles could be the intraoperative evaluation of tumor resection margins.

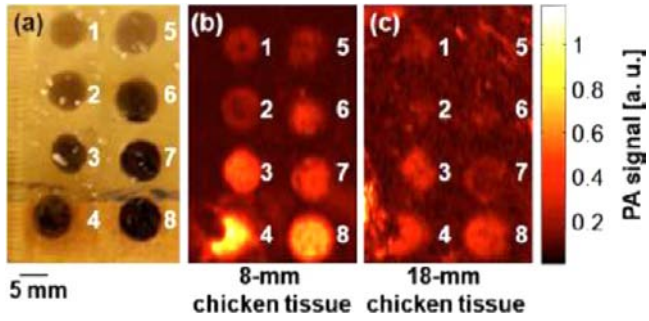

Figure 10. (a) Photograph of a phantom containing tumor simulators made of ink-encapsulated MBs and NBs with various concentrations. (b) Corresponding PA image of the phantom positioned below 8 mm of chicken breast tissues. (c) Corresponding PA image of the phantom positioned below 18 mm of chicken breast tissues. 1−4: MBs at concentrations of 2.5, 5.0, 10, and 15 mg/mL, respectively. 5−8: NBs at concentrations of 2.5, 5.0, 10, and 15 mg/mL, respectively. Reprinted with permission from ref 73.

US/CT/MR Trimodal Imaging Agents. Apart from dual-modal imaging agents, several different contrast agents for US, CT, and MR trimodal imaging were developed by the Bulte group. PFOB NPs, which can be detected by ^{19}F MRI, US imaging, and CT, were used to label human cadaveric islets for the *in vivo* trimodal imaging of engraftment and immunorejection of transplanted islets.[74] Similarly, PFOB emulsion was incorporated into alginate microcapsules to image the encapsulation and immunoisolation of cellular therapeutics by

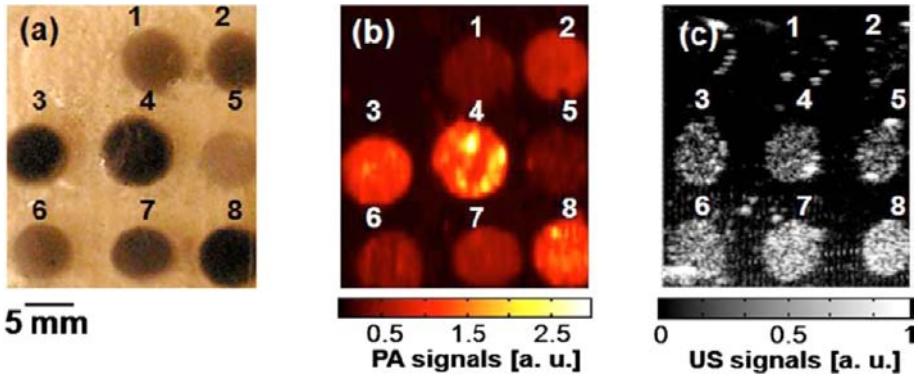

Figure 9. (a) Photograph of a phantom containing tumor simulators made of ink-encapsulated MBs and NBs with various concentrations. (b) Corresponding PA image. (c) Corresponding US image. 1−4: MBs at concentrations of 2.5, 5.0, 10, and 15 mg/mL, respectively. 5−8: NBs at concentrations of 2.5, 5.0, 10, and 15 mg/mL, respectively. Reprinted with permission from ref 73.

dx.doi.org/10.1021/bc500092h | *Bioconjugate Chem.* 2014, 25, 840−854

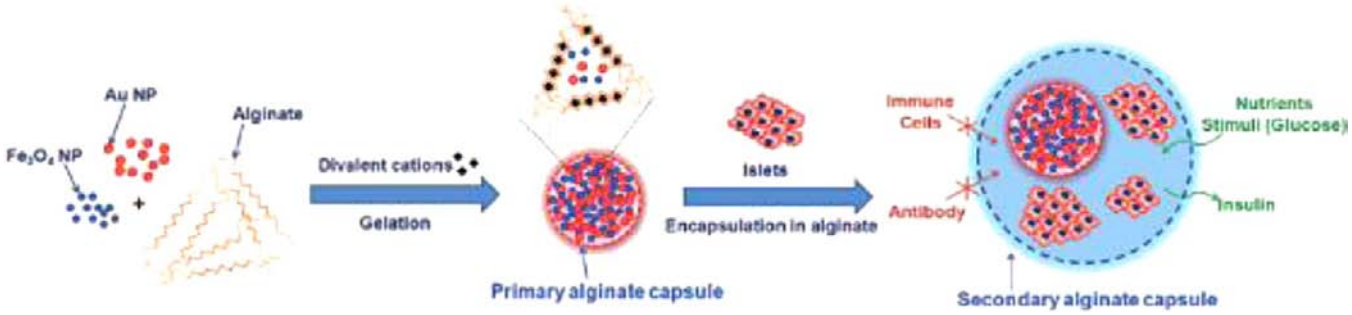

Figure 11. Schematic representation of the composition of the "capsule-in-capsules": the primary capsule contains iron oxide and gold NPs, while the secondary-capsule contains islet cells. Reprinted with permission from ref 76.

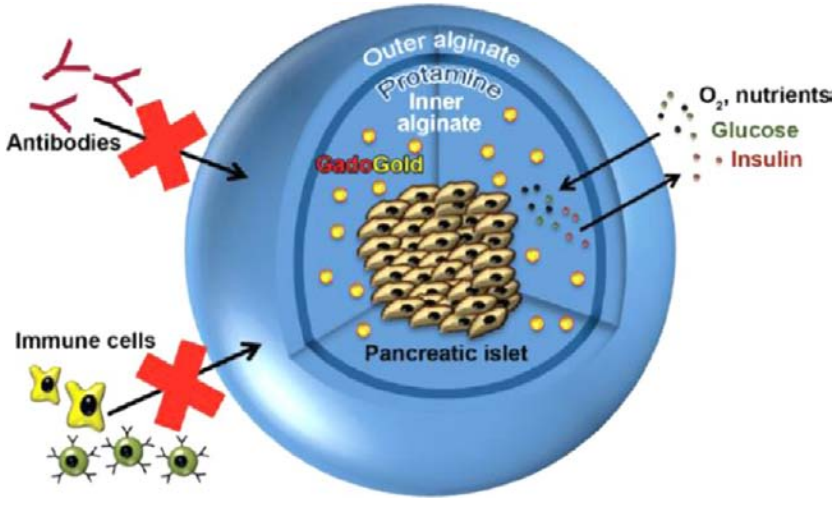

Figure 12. Three-dimensional scheme of alginate-protamine sulfate-alginate microcapsule containing gadolinium chelates. The semipermeable microcapsule allows diffusion of oxygen, nutrients, glucose, and insulin, while passage of immune cells and antibodies is blocked. Reprinted with permission from ref 77.

^{19}F MRI, X-ray, and US techniques.[75] Additionally, this group has synthesized a "capsule-in-capsules" by encapsulating gold, iron oxide NPs, and islet cells in a primary inner capsule within the secondary outer capsule (Figure 11), and they demonstrated that the "capsule-in-capsules" can be tracked with three modalities, i.e., MR, CT, and US imaging.[76] Another report by the same group showed the coencapsulation of gold NPs that were functionalized with dithiolated diethylenetriaminepentaacetic acid:gadolinium chelates with human pancreatic islets into alginate-protamine sulfate-alginate capsules,[77] as represented in Figure 12. These microcapsules containing pancreatic cells provide a versatile means for noninvasively monitoring engrafted capsules in real time, and they hold potential for treating type I diabetes without immunosuppressive therapy.

Although the integration of other imaging modalities with US is expected to provide more precise and detailed information for clear diagnosis than US alone, the rational selection of imaging modalities for multimodal imaging is highly important. During the design of US-based multimodal imaging probes, researchers should avoid the overlap of advantages and instead compensate for the weak points of each modality to maximize the synergistic effect. This is the reason that the real-time and noninvasive US imaging but with low sensitivity, and spatial resolution is frequently combined with other imaging modalities with high spatial resolution (MR, CT, etc.) or high sensitivity (optical, etc.). Although different imaging techniques are thought to compensate for one another, there is still concern over the different sensitivity of each modality. For example, NIR fluorescence agents can be used at extremely low concentrations, while MR and CT agents require relatively high concentrations. Therefore, it is necessary to take into account the total dosage of the contrast agents and the amounts of each imaging agent when two or more imaging instruments are fused together. Improving imaging instruments is expected to alleviate these problems by providing fine images with small numbers of probes.

■ ULTRASOUND CONTRAST AGENTS FOR IMAGING GUIDED PHOTOTHERMAL THERAPY

The term "theranostics" comprises two distinct definitions: specific, individualized therapies for various diseases and the combination of diagnostic and therapeutic agents into a single platform. We currently focus on the latter. The emergence of multifunctional theranostic agents offered an opportunity to draw diagnosis and therapy closer and shortened treatment and hospital stay times. Diagnostic UCAs can be readily "upgraded" to theranostic agents by outfitting therapeutic functions on them. MB carriers are uniquely suitable for ultrasound-enhanced local drug delivery because they can be selectively concentrated and destroyed at the acoustic focal regions. With the aid of an imaging agent, the biodistribution of UCAs or drugs, the accumulation at the target sites, as well as the therapeutic results, can be confirmed noninvasively under *in vivo* conditions. Because many review papers on UCAs for

drug/gene delivery[78−82] and thrombolysis[83,84] have been published, herein we will primarily focus on recent advances in employing UCA as a novel theranostic agent in US imaging guided photothermal therapy.

US Imaging Guided Photothermal Therapy. Recent advances in nanotechnology have provided a range of novel materials that act as photothermal agents, such as gold nanomaterials (gold nanorods, gold nanocages, and gold nanoshells),[85−88] carbon nanomaterials (carbon nanotubes, graphene, and nanohorns),[89−93] CuS NPs,[94] Prussian blue NPs,[95] and polypyrrole NPs,[96] and so forth. Among these options, gold nanostructures exhibit good biocompatibility in addition to excellent optical and electronic properties, thus allowing their use in biological and medical fields. The first report on US imaging combined photothermal therapy that was composed of PLA microcapsules (MCs) and NIR-absorbing gold nanoshells (GNS) or GNRs was demonstrated by our group.[39,97] *In vivo* ultrasound imaging evaluation showed that the modification of GNS or GNRs did not weaken the acoustic properties of the microcapsules, and the HeLa cells incubated with the theranostic agents could be killed selectively by NIR light-induced photothermal effect (Figure 13). Thus, the dual-functional gold-PLA composites were shown to operate ultrasound-guided photothermal tumor therapy.

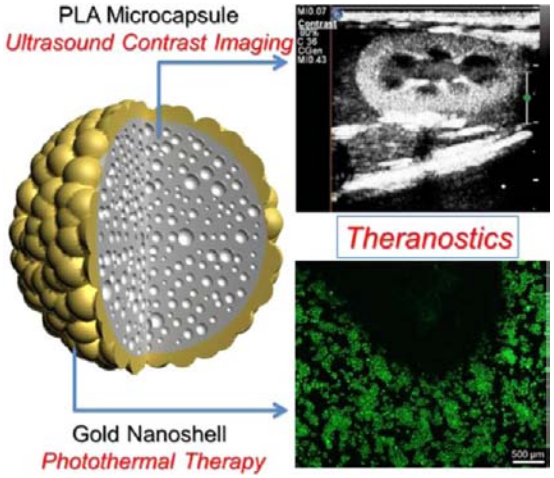

Figure 13. Gold nanoshelled microcapsules operate as a novel theranostic agent for both contrast-enhanced ultrasonic imaging and photohyperthermia. (Scale bars: 500 mm; GNS-MCs agent concentration: 0.3 mg mL^{-1}; NIR laser: 808 nm, 8 W cm^{-2}, 10 min). Reprinted with permission from ref 97.

To accomplish more efficient photothermal tumor ablation, we upgraded gold nanoshelled microcapsules to nanoscaled theranostic agents by incorporating two extra components of SPIOs and PFOB into PLA nanocapsules with an additional PEGylation (Figure 14a).[98] The resulting PEGylated gold nanoshell nanocapsule-entrapping SPIO NPs and PFOB (PGS-SP NC) exhibited a rough surface morphology and an average diameter of approximately 373.6 nm (Figure 14b). PGS-SP NCs not only could be used to guide US contrast imaging (Figure 14c), but were also applicable to MRI guidance (Figure 14d). With the help of US imaging, the distribution of the photoabsorber can be ensured to guide the following photoablation therapy. The MR contrast imaging displayed the xenografted tumor as a gray area inside a red circle before the intravenous administration of the nanocapsule suspension. However, the tumor was darkened by 0.5 h later, suggesting the SPIO-functionalized nanocapsules had been aggregated in the tumor site to generate negative contrast in the T_2-weighted MR image. After the agent was injected intravenously into the tumor-bearing mice, the nanocapsules tended to accumulate in the tumor sites because of an enhanced permeability and retention effect, which was enhanced by the nanoscaled size and surface PEGylation of the nanocapsules.

In HT-1080 tumor-bearing nude mice, the tumor size was deceased by 34.0% on the ninth day after treating with an intravenous injection of PGS-SP NCs followed by NIR laser irradiation, but there was no significant difference in the final tumor size relative to the control groups.

Gold nanoshelled NCs could also serve as effective CT contrast agents.[99] Thus, the relatively poor spatial and anatomical resolution of US images might be overcome by the integration of MRI and CT, which have excellent spatial and anatomical resolution. This type of single theranostic agent in combination with real-time US and high-resolution MR and CT imaging would be of great value in generating more comprehensive information about the diagnosis and dynamics of disease progression, which could be used for the accurate location of therapeutic focusing spots in the targeted tumor tissue. This technique exhibits great potential as an effective nanoplatform for contrast imaging-guided photothermal therapy.

Because of the d−d transition of Cu^{2+} ions, CuS NPs show strong NIR absorption, which is unaffected by the solvent or the surrounding environment when CuS NPs are formulated or delivered *in vivo*.[100] Thus, a novel microbubble system was developed for both ultrasound imaging and targeted CuS NPs delivery by using UTMD to kill tumor cells with the photothermal effect.[101] The composite MBs were fabricated by depositing photothermal CuS NPs onto the outer surface of gas-filled ST68 MBs (CuS-ST68 MBs). In addition to their outstanding ultrasound imaging capability, "soft" CuS-ST68 MBs would cavitate violently under the UTMD effect and then release the CuS NPs, which could penetrate into the tumor interstitium to kill the tumor cells with the aid of NIR light irradiation. Nanoshelled microcapsules would stay in the tumor vasculature rather than penetrate into the tumor interstitium because of their relatively large size, which may result in the insufficient ablation of tumor cells. However, the smaller CuS NPs are more probable for reaching their targets and being cleared from the body through the renal system.[100,102,103]

When compared with NIR-absorbing inorganic components, which are nonbiodegradable and thus show potential long-term toxicity, organic compounds have attracted great interest over various photothermal therapy studies.[104,105] Very recently, polypyrrole (PPy) nanoparticles have been given more attention during photothermal ablation therapy owing to their strong NIR absorption property.[106,107] PPy nanoparticles have good biocompatibility with the photothermal ablation therapy of cancer; moreover, when compared with Au nanorods, PPy nanoparticles exhibit higher photothermal conversion efficiency and NIR photostability.[96] PFOB was recently encapsulated into the soluble PPy complex to prepare water-dispersible PPy nano/microcapsules by easily tuning the synthesis parameters. Because of the favorable NIR-absorbing property of the PPy shell and the good echogenicity of the PFOB core, the resulting PFOB-loaded PPy nano- and microcapsules operated as an excellent multifunctional photothermal agent for a real-time US imaging-guided photothermal

dx.doi.org/10.1021/bc500092h | *Bioconjugate Chem.* 2014, 25, 840−854

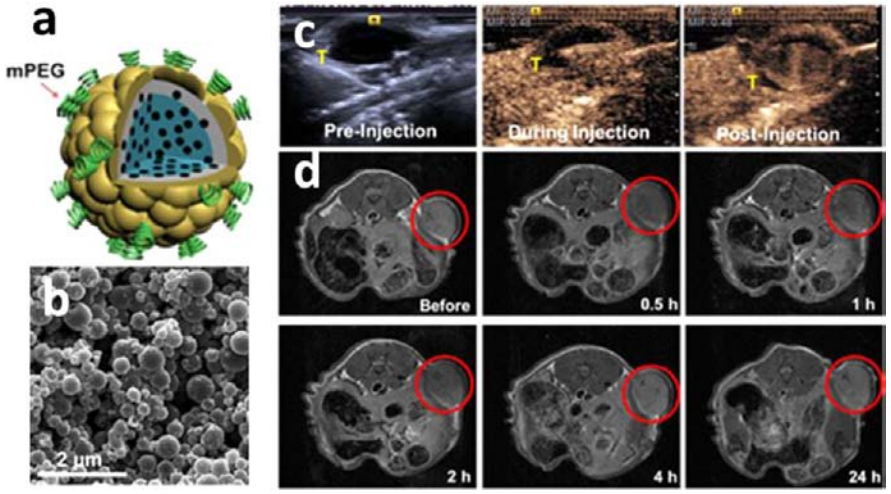

Figure 14. (a) Schematic PEGylated gold nanoshell nanocapsule entrapping SPIO NPs and PFOB (PGS-SP NC). (b) SEM images of the PGS-SP NPs. (c) Contrast-enhanced ultrasonograms before, during, and after the intratumoral injection of the agent (0.2 mL, 2 mg mL^{-1}) into the mice for visualization of the agent distribution to guide the following therapy (tumors highlighted by T). (d) T_2-weighted MR images of the tumors at different time points after intravenous injection of the agent (0.15 mL, 2 mg mL^{-1}) for visualization of tumor areas to guide the following photothermal ablation (tumors are highlighted in the red circles). Reprinted with permission from ref 98.

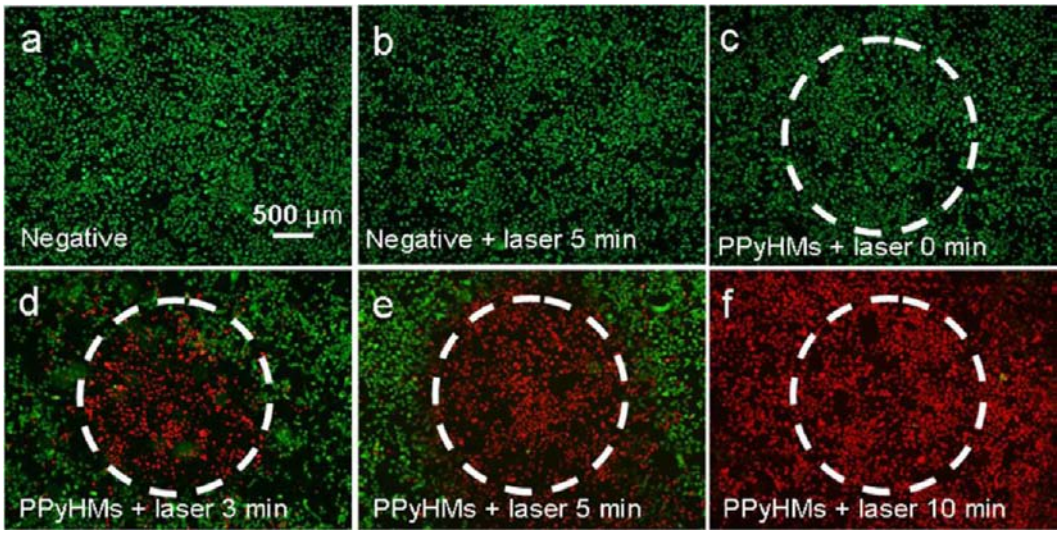

Figure 15. Localized photohyperthermic effect. Photothermal destruction of U87-MG cells with or without PPyHMs and NIR laser (808 nm, 6 W cm^{-2}) treatments (a, b, c, d, e, and f). White circle indicates the laser spot; live/dead stain for viability shows dead cells as red while viable cells as green. Reprinted with permission from ref 108.

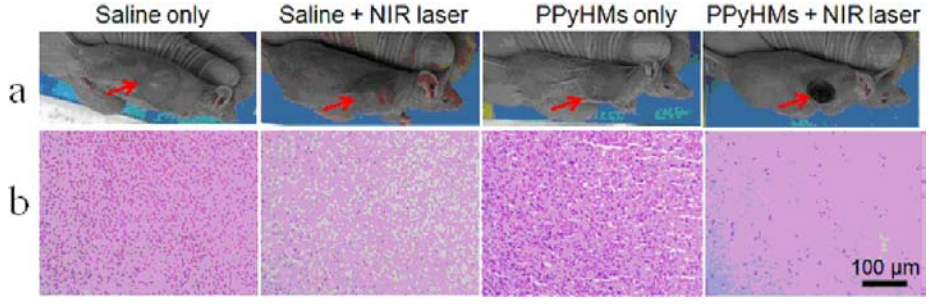

Figure 16. (a) Representative photographs of mice bearing U87-MG tumors after various different treatments indicated. (b) H&E stained tumor slices collected from different groups of mice immediately after laser irradiation. The PPyHMs injected tumor was severely damaged after laser irradiation. Reprinted with permission from ref 108.

treatment of cancer cells.[108] In addition to ablating tumor upon NIR light irradiation, PPy material can also provide excellent contrast enhancement for US imaging. Very recently, our group fabricated PPy hollow microspheres (PPyHMs) by using a

dx.doi.org/10.1021/bc500092h | Bioconjugate Chem. 2014, 25, 840−854

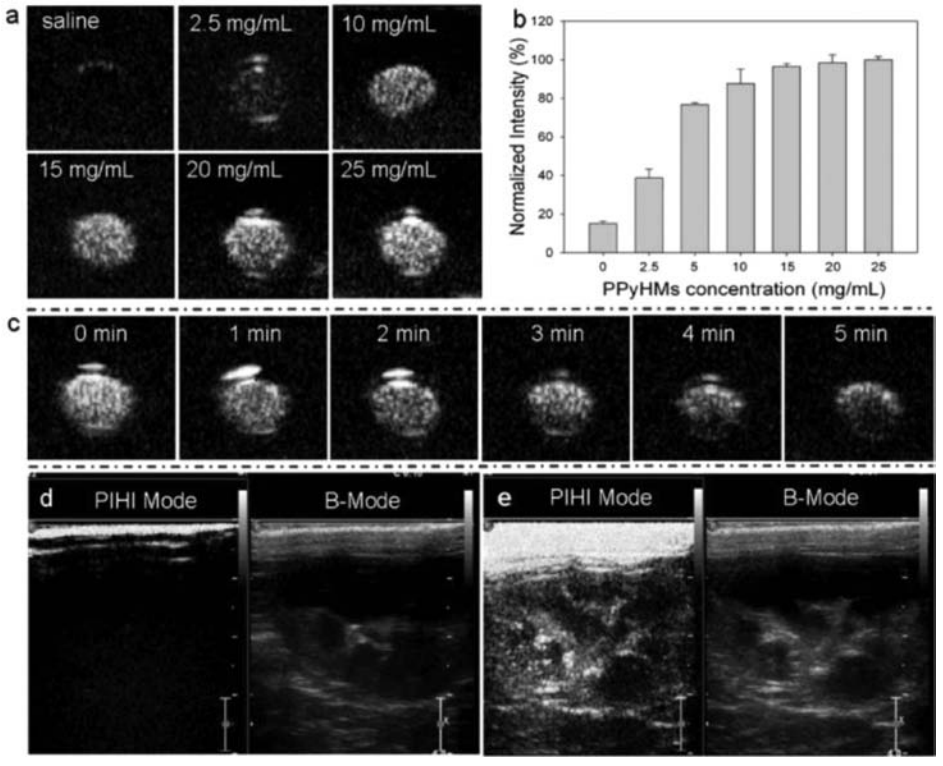

Figure 17. *In vitro* ultrasound contrast-enhanced images in a latex tube: (a) US images of various concentrations of PPyHMs. (b) Normalized US intensities over PPyHMs concentration. (c) Time-dependent echogenic behaviors of PPyHMs at the concentration of 20 mg mL^{-1}. *In vivo* ultrasonograms in the rabbit right kidney (d) pre- and (e) postadministration of PPyHMs. Reprinted with permission from ref 108.

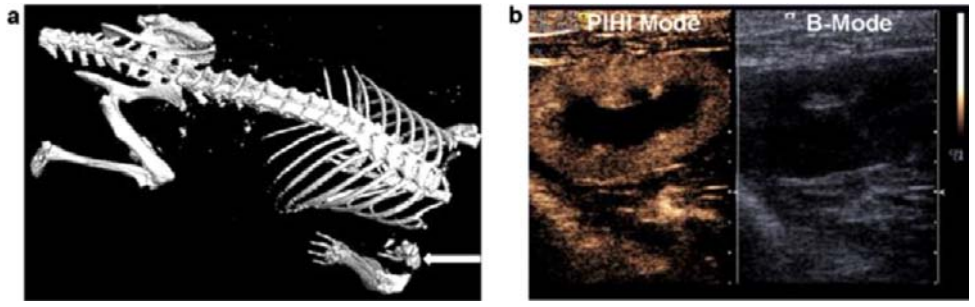

Figure 18. *In vivo* X-ray CT imaging of mice after intramuscular injection of Au@PLA-$(PAH/GO)_2$ microcapsules (the white arrow points to the microcapsule-injected region). (b) *In vivo* ultrasonograms in the rabbit right kidney after administration of the microcapsule of Au@PLA-$(PAH/GO)_2$. Reprinted with permission from ref 111.

simple oil-in-water microemulsion method.[109] The PPyHMs caused a significant photothermal therapeutic effect, and 80% of the U87-MG cells died when they were incubated with 7 μg mL^{-1} PPyHMs under NIR laser irradiation (Figure 15). *In vivo* experiments showed that the tumor volume was effectively decreased after PPyHM injection and laser exposure (Figure 16a). Hematoxylin and eosin staining in tumor slices indicated significant cancer cell damage (Figure 16b). Importantly, because of the hollow structure, PPyHMs displayed excellent US contrast-enhancing ability both *in vitro* and *in vivo*, as shown in Figure 17. The construction of PPyHMs successfully combined US imaging and photothermal therapy with no need for additional NIR-absorbing agents, reduced the high onetime dose, and prevented the change in the shell stiffness. Consequently, PPyHMs show great prospect as a new generation of theranostic agent for US imaging guided photothermal therapy. In addition, PPy was found to be a new type of contrast agent for photoacoustic imaging, with good biocompatibility, high spatial resolution, and enhanced sensitivity.[110] Undoubtedly, PPy is a versatile material, exhibiting great prospects for enhancing US imaging, photoacoustic imaging, and imaging-guided photothermal therapy.

US/CT Bimodal Imaging Guided Photothermal Therapy. The clinical application of the ACUSON S3000 ultrasound system combining real-time US and 3-D CT has triggered great interest in designing multifunctional contrast agents for US/CT biomodal imaging or theranostic agents for US/CT biomodal imaging-guided therapy. Recently, a new type of theranostic MCs were successfully fabricated by our group for photothermal tumor destruction under the guidance of US/CT bimodal imaging by introducing gold NPs into PLA microcapsules through a double-microemulsion method, followed by depositing graphene oxide (GO) onto the microcapsule surface via an electrostatic layer-by-layer self-assembly technique.[111] Au NPs act as contrast agents to

dx.doi.org/10.1021/bc500092h | *Bioconjugate Chem.* 2014, 25, 840−854

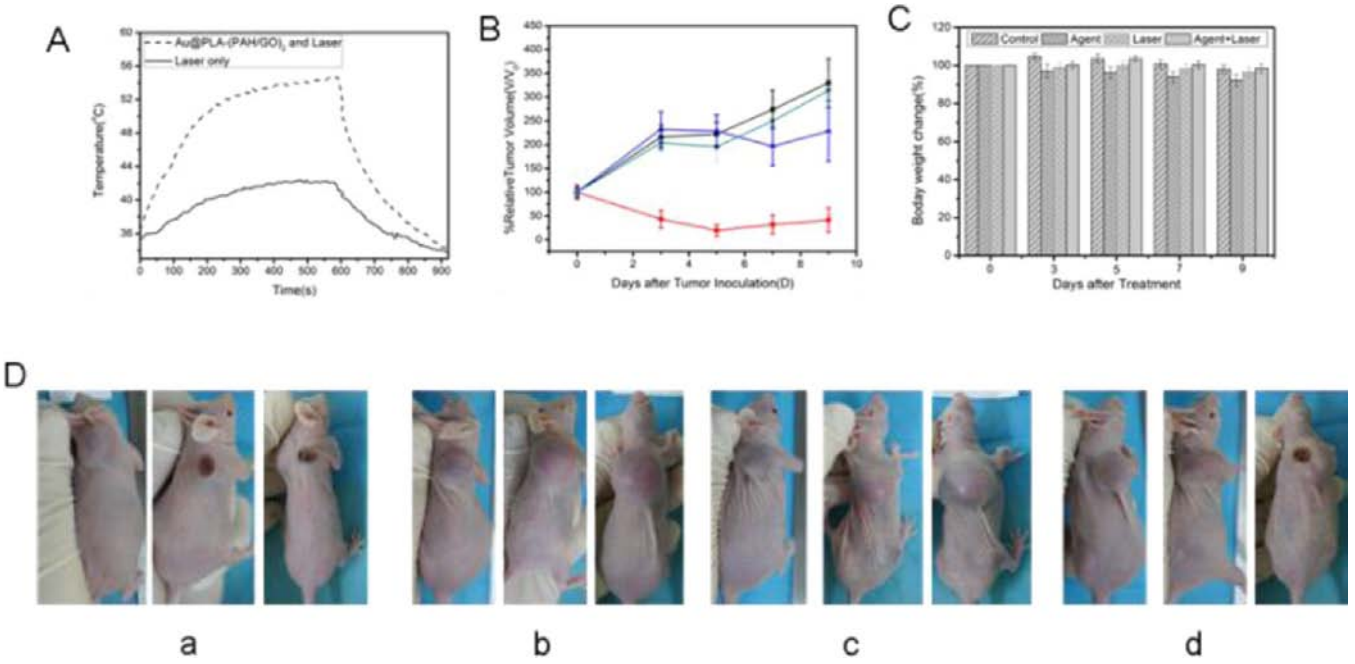

Figure 19. (A) Temperature change curves determined by thermographic camera after treatments of the nude mice tumor with saline or Au@PLA-$(PAH/GO)_2$ microcapsules upon exposure to the 808 nm laser at a power density of 2.23 W/cm^2. (B) Quantitative measurement of tumor volume in mice after different treatments. The tumor volumes were normalized to their initial sizes (■ saline solution, ● Au@PLA-$(PAH/GO)_2$ microcapsules + Laser, ▼ saline solution + Laser, ▲ Au@PLA-$(PAH/GO)_2$ microcapsules). (C) Body weights of mice at different time points after various treatments. (D) Representative photographs of tumors in mice before and after various treatment for 1 days and 6 days (a, Au@PLA-$(PAH/GO)_2$ microcapsules + Laser; b, saline solution; c, Au@PLA-$(PAH/GO)_2$ microcapsules only; d, saline solution + Laser). Reprinted with permission from ref 111.

enhance CT imaging, and GO is used as a strong NIR-light absorbing agent for the photothermal ablation of cancer.

In vivo CT and US imaging experiments showed that the resulting MCs could serve as a contrast agent to enhance X-ray CT imaging and US imaging simultaneously (Figure 18). In addition, the tumor growth was inhibited of 83.8% in the presence of near-infrared light and MCs within 9 days (Figure 19). Such a versatile MC system might bring novel opportunities to the next generation of multimodal imaging-guided cancer therapy.

US/PA Bimodal Imaging-Guided Photothermal Therapy. US and PA are both noninvasive and nonradioactive imaging tools. Because they share the same instrumentation, US and PA modalities are commonly paired with each other and provide complementary information as a potent dual-modality method. US/PA dual-modality contrast agents can be prepared by combining UCA with an optical absorption substance. Specifically, if the optical absorption substance can serve as a therapeutic species in addition to enhancing the PA signals, US/PA dual-modality imaging with combination of therapy can be achieved simultaneously. A US/PA dual-modality contrast agent composed of human serum albumin-shelled MBs and gold nanorods was recently proposed.[38] The gold nanorods were used as NIR light absorbers to enhance the PA signals and generate a photothermal effect. More recently, we successfully constructed a multifunctional ultrasound contrast agent by encapsulating SPIO NPs into the PLA microcapsules via a double emulsion evaporation process followed by GO deposition onto the microcapsule surface.[112] The resulting composite agents not only provided prominent contrast enhancement for the trimodality imaging of US/MR/PA, but also served as efficient NIR photoabsorbers for the photothermal ablation of cancer cells upon NIR laser irradiation without damaging normal cells. Moreover, this photothermal effect was obviously enhanced by applying an external magnetic field because of the presence of SPIO NPs inside the microcapsules. This contrast-enhanced US/MR/PA trimodal imaging guidance could display dynamic complementary information about the tumors to help alter the treatment through personalization and high efficiency. This type of multifunctional agent is anticipated to foster innovative avenues for developing multifunctional platforms for cancer diagnosis and treatments.

Admittedly, the combination of US imaging and photothermal therapy will have great potential as theranostic agents in clinics because of their safety and site-specific therapy. However, many important problems still remain unresolved; for example, the payload of MBs is restricted because the effective carrying capability is limited to their shell; the circulation time of MBs is only a few minutes; the stability of MBs might be decreased when encapsulating photothermal NPs; and it is unclear how to maintain an adequate acoustic capability of photothermal NPs-loaded MBs, and so forth. Moreover, for US imaging guided photothermal therapy, the identification of the location and size of the tumor before therapy is important to avoid damage from the NIR light to normal cells. Thus, it is necessary to construct active-targeted MBs by incorporating ligands onto the membrane of MBs. In addition, the penetration depth of NIR light restricts its application in superficial tumors, and the deep-seated tumors must be aided by interventional therapy that inserts an optical fiber into the specific site. Anyway, US imaging guided photothermal tumor ablation therapy is believed to be a promising field in cancer

treatment, and the above issues will be solved with the development of biotechnology and materials science.

CONCLUSION AND PERSPECTIVE

Despite the tremendous advances of US-based multifunctional imaging and theranostic agents in preclinical diagnosis and therapy, examples of these investigations are rare to date, and they primarily focus on US/MRI dual-functional contrast agents or drug or gene delivery systems. Moreover, the present studies are still restricted to simulated investigations, cell investigations, and small animal studies.[113] The emergence of nanotechnology has endowed traditional US imaging with new abilities for integrated diagnosis and image-guided therapy. Various NPs, such as QDs, Fe_3O_4, Bi_2S_3, gold, CuS, and carbon materials, and so forth, possess unique optical, magnetic, X-ray absorbing, or photothermal properties and have achieved great success in the imaging or therapeutic fields. These techniques have laid the foundation for current studies because the probes can easily be upgraded when combined with ultrasonic MBs. Future studies should focus on the development of highly stable, biocompatible, targeted multifunctional, ultrasound imaging, and therapeutic agents, and accelerate their clinical translation.

AUTHOR INFORMATION

Corresponding Author

*E-mail: zhifei.dai@pku.edu.cn. Homepage: http://bme.pku.edu.cn/~daizhifei.

Notes

The authors declare no competing financial interest.

ACKNOWLEDGMENTS

This work was financially supported by the National Natural Science Foundation of China (No. 81101094), the National Natural Science Foundation for Distinguished Young Scholars (No. 81225011), and the State Key Program of National Natural Science of China (Grant No. 81230036).

ABBREVIATIONS

UCAs, ultrasound contrast agents; MBs, microbubbles; MRI, magnetic resonance imaging; CT, computer tomography; PET, positron emission tomography; UTMD, ultrasound targeted microbubble destruction; PLA, poly(lactic acid); PEG, poly(ethylene glycol); PLGA, poly(lactide-*co*-glycolide acid); PVA, poly(vinyl alcohol); SPIO, superparamagnetic iron oxide; QDs, quantum dots; ICG, indocyanine green; GNRs, gold nanorods; VEGFR2, vascular endothelial growth factor receptor 2; NBs, nanobubbles; PA, photoacoustic; PFC, perfluorocarbon; PAnDs, photoacoustic nanodroplets; HIFU, high intensity focused ultrasound; PFH, perfluorohexane; MSNCs, mesoporous silica nanocapsules; NIR, near-infrared region; MCs, microcapsules; GNS, gold nanoshells; PPyHMs, PPy hollow microspheres; GO, graphene oxide

REFERENCES

(1) Park, J. I., Jagadeesan, D., Williams, R., Oakden, W., Chung, S., Stanisz, G. J., and Kumacheva, E. (2010) Microbubbles loaded with nanoparticles: a route to multiple imaging modalities. *ACS Nano 4*, 6579−6586.

(2) Stride, E., and Edirisinghe, M. (2008) Novel microbubble preparation technologies. *Soft Matter 4*, 2350−2359.

(3) Zhang, Y., Yang, Y. A., and Cai, W. B. (2011) Multimodality Imaging of Integrin alpha(v)beta(3) Expression. *Theranostics 1*, 135−148.

(4) Kiessling, F., Gaetjens, J., and Palmowski, M. (2011) Application of molecular ultrasound for imaging integrin expression. *Theranostics 1*, 127−134.

(5) Feinstein, S. B., Ten Cate, F. J., Zwehl, W., Ong, K., Maurer, G., Tei, C., Shah, P. M., Meerbaum, S., and Corday, E. (1984) Two-dimensional contrast echocardiography. I. In vitro development and quantitative analysis of echo contrast agents. *J. Am. Coll. Cardiol. 3*, 14−20.

(6) El-Sherif, D. M., and Wheatley, M. A. (2003) Development of a novel method for synthesis of a polymeric ultrasound contrast agent. *J. Biomed. Mater. Res., Part A 66*, 347−355.

(7) Straub, J. A., Chickering, D. E., Church, C. C., Shah, B., Hanlon, T., and Bernstein, H. (2005) Porous PLGA microparticles: AI-700, an intravenously administered ultrasound contrast agent for use in echocardiography. *J. Controlled Release 108*, 21−32.

(8) Leong-Poi, H., Christiansen, J., Heppner, P., Lewis, C. W., Klibanov, A. L., Kaul, S., and Lindner, J. R. (2005) Assessment of endogenous and therapeutic arteriogenesis by contrast ultrasound molecular imaging of integrin expression. *Circulation 111*, 3248−3254.

(9) Rychak, J. J., Lindner, J. R., Ley, K., and Klibanov, A. L. (2006) Deformable gas-filled microbubbles targeted to P-selectin. *J. Controlled Release 114*, 288−299.

(10) Basude, R., Duckworth, J. W., and Wheatley, M. A. (2000) Influence of environmental conditions on a new surfactant-based contrast agent: ST68. *Ultrasound Med. Biol. 26*, 621−628.

(11) Takeuchi, S., Sato, T., and Kawashima, N. (2002) Non-linearresponse of microbubblescoated with surfactantmembrane developed as ultrasound contrast agent—experimental study and numerical calculations. *Colloids Surf., B 24*, 207−216.

(12) Nolsoe, C. P., Torp-Pedersen, S., Burcharth, F., Horn, T., Pedersen, S., Christensen, N. E., Olldag, E. S., Andersen, P. H., Karstrup, S., and Lorentzen, T. (1993) Interstitial hyperthermia of colorectal liver metastases with a US-guided Nd-YAG laser with a diffuser tip: a pilot clinical study. *Radiology 187*, 333−337.

(13) Amin, Z., Donald, J. J., Masters, A., Kant, R., Steger, A. C., Bown, S. G., and Lees, W. R. (1993) Hepatic metastases: interstitial laser photocoagulation with real-time US monitoring and dynamic CT evaluation of treatment. *Radiology 187*, 339−347.

(14) Weissleder, R. (2001) A clearer vision for in vivo imaging. *Nat. Biotechnol. 19*, 316−317.

(15) Unger, E. C., McCreery, T. P., Sweitzer, R. H., Caldwell, V. E., and Wu, Y. (1998) Acoustically active lipospheres containing paclitaxel: a new therapeutic ultrasound contrast agent. *Invest. Radiol. 33*, 886−892.

(16) Zhao, Y. Z., Liang, H. D., Mei, X. G., and Halliwell, M. (2005) Preparation, characterization and in vivo observation of phospholipid-based gas-filled microbubbles containing hirudin. *Ultrasound Med. Biol. 31*, 1237−1243.

(17) Christiansen, C., Kryvi, H., Sontum, P. C., and Skotland, T. (1994) Physical and biochemical characterization of Albunex, a new ultrasound contrast agent consisting of air-filled albumin microspheres suspended in a solution of human albumin. *Biotechnol. Appl. Biochem. 19* (Pt 3), 307−320.

(18) Bjerknes, K., Dyrstad, K., Smistad, G., and Agerkvist, I. (2000) Preparation of polymeric microcapsules: formulation studies. *Drug Dev. Ind. Pharm. 26*, 847−856.

(19) Jiang, B. B., Gao, C. Y., and Shen, J. C. (2006) Polylactide hollow spheres fabricated by interfacial polymerization in an oil-in-water emulsion system. *Colloid Polym. Sci. 284*, 513−519.

(20) Masato Kukizakia, M. G. (2007) Spontaneous formation behavior of uniform-sized microbubbles from Shirasu porous glass (SPG) membranes in the absence of water-phase flow. *Colloids Surf., A 296*, 174−181.

(21) Böhmer, M. R., Schroeders, R., Steenbakkers, J. A. M., de Winter, S. H. P. M., Duineveld, P. A., Lub, J., Nijssen, W. P. M., Pikkemaat, J. A., and Stapert, H. R. (2006) Preparation of

monodisperse polymer particles and capsules by ink-jet printing. *Colloids Surf., A 289*, 96−104.
(22) Farook, U., Zhang, H. B., Edirisinghe, M. J., Stride, E., and Saffari, N. (2007) Preparation of microbubble suspensions by co-axial electrohydrodynamic atomization. *Med. Eng. Phys. 29*, 749−754.
(23) Farook, U., Stride, E., Edirisinghe, M. J., and Moaleji, R. (2007) Microbubbling by co-axial electrohydrodynamic atomization. *Med. Biol. Eng. Comput. 45*, 781−789.
(24) Whitesides, G. M. (2006) The origins and the future of microfluidics. *Nature 442*, 368−373.
(25) Pancholi, K. P., Farook, U., Moaleji, R., Stride, E. M., and Edirisinghe, J. (2008) Novel methods for preparing phospholipid coated microbubbles. *Eur. Biophys. J. 37*, 515−520.
(26) Xing, Z. W., Ke, H. T., Wang, J. R., Zhao, B., Yue, X. L., Dai, Z. F., and Liu, J. B. (2010) Novel ultrasound contrast agent based on microbubbles generated from surfactant mixtures of span 60 and polyoxyethylene 40 stearate. *Acta Biomater. 6*, 3542−3549.
(27) Cui, W., Bei, J., Wang, S., Zhi, G., Zhao, Y., Zhou, X., Zhang, H., and Xu, Y. (2005) Preparation and evaluation of poly(L-lactide-co-glycolide) (PLGA) microbubbles as a contrast agent for myocardial contrast echocardiography. *J. Biomed. Mater. Res., Part B 73*, 171−178.
(28) El-Sherif, D. M., Lathia, J. D., Le, N. T., and Wheatley, M. A. (2004) Ultrasound degradation of novel polymer contrast agents. *J. Biomed. Mater. Res., Part A 68*, 71−78.
(29) Wheatley, M. A., Lathia, J. D., and Oum, K. L. (2007) Polymeric ultrasound contrast agents targeted to integrins: Importance of process methods and surface density of ligands. *Biomacromolecules 8*, 516−522.
(30) Frenkel, P. A., Chen, S., Thai, T., Shohet, R. V., and Grayburn, P. A. (2002) DNA-loaded albumin microbubbles enhance ultrasound-mediated transfection in vitro. *Ultrasound Med. Biol. 28*, 817−822.
(31) Soetanto, K., and Hiroshi, W. (2000) Development of magnetic microbubbles for drug delivery system (DDS). *Jpn. J. Appl. Phys. 39*, 3230−3232.
(32) Yang, F., Li, Y., Chen, Z., Zhang, Y., Wu, J., and Gu, N. (2009) Superparamagnetic iron oxide nanoparticle-embedded encapsulated microbubbles as dual contrast agents of magnetic resonance and ultrasound imaging. *Biomaterials 30*, 3882−3890.
(33) Chow, A. M., Chan, K. W., Cheung, J. S., and Wu, E. X. (2010) Enhancement of gas-filled microbubble R2* by iron oxide nanoparticles for MRI. *Magn. Reson. Med. 63*, 224−229.
(34) Liu, Z., Lammers, T., Ehling, J., Fokong, S., Bornemann, J., Kiessling, F., and Gatjens, J. (2011) Iron oxide nanoparticle-containing microbubble composites as contrast agents for MR and ultrasound dual-modality imaging. *Biomaterials 32*, 6155−6163.
(35) Brismar, T. B., Grishenkov, D., Gustafsson, B., Harmark, J., Barrefelt, A., Kothapalli, S. V., Margheritelli, S., Oddo, L., Caidahl, K., Hebert, H., and Paradossi, G. (2012) Magnetite nanoparticles can be coupled to microbubbles to support multimodal imaging. *Biomacromolecules 13*, 1390−1399.
(36) Ke, H. T., Xing, Z. W., Zhao, B., Wang, J. R., Liu, J. B., Guo, C. X., Yue, X. L., Liu, S. Q., Tang, Z. Y., and Dai, Z. F. (2009) Quantum-dot-modified microbubbles with bi-mode imaging capabilities. *Nanotechnology 20*, 425105.
(37) Xu, R. X., Huang, J., Xu, J. S., Sun, D., Hinkle, G. H., Martin, E. W., and Povoski, S. P. (2009) Fabrication of indocyanine green encapsulated biodegradable microbubbles for structural and functional imaging of cancer. *J. Biomed. Opt. 14*, 034020.
(38) Wang, Y. H., Liao, A. H., Chen, J. H., Wang, C. R., and Li, P. C. (2012) Photoacoustic/ultrasound dual-modality contrast agent and its application to thermotherapy. *J. Biomed. Opt. 17*, 045001.
(39) Ke, H. T., Wang, J. R., Dai, Z. F., Jin, Y. S., Qu, E. Z., Xing, Z. W., Guo, C. X., Liu, J. B., and Yue, X. L. (2011) Bifunctional gold nanorod-loaded polymeric microcapsules for both contrast-enhanced ultrasound imaging and photothermal therapy. *J. Mater. Chem.*, 5561−5564.
(40) Seo, M., Gorelikov, I., Williams, R., and Matsuura, N. (2010) Microfluidic assembly of monodisperse, nanoparticle-incorporated perfluorocarbon microbubbles for medical imaging and therapy. *Langmuir 26*, 13855−13860.
(41) Townsend, D. W. (2008) Multimodality imaging of structure and function. *Phys. Med. Biol. 53*, R1−R39.
(42) Hendee, W. R., and G, S. (2006) Biomedical imaging research opportunities workshop III: a white paper. *Ann. Biomed. Eng. 34*, 188−198.
(43) Hendee, W. R., Banovac, F., Carson, P. L., DeFronzo, R. A., Eckelman, W. C., Fullerton, G. D., Larson, S. M., McLennan, G., and Welch, M. J. (2007) Biomedical imaging research opportunities workshop IV: a white paper. *Med. Phys. 34*, 673−679.
(44) Louie, A. (2010) Multimodality imaging probes: design and challenges. *Chem. Rev. 110*, 3146−3195.
(45) Arditi, M., Frinking, P. J., Zhou, X., and Rognin, N. G. (2006) A new formalism for the quantification of tissue perfusion by the destruction-replenishment method in contrast ultrasound imaging. *IEEE Transactions on Ultrasonics, Ferroelectrics, and Frequency Control 53*, 1118−1129.
(46) Lindner, J. R., Song, J., Jayaweera, A. R., Sklenar, J., and Kaul, S. (2002) Microvascular rheology of definity microbubbles after intra-arterial and intravenous administration. *J. Am. Soc. Echocardiogr. 15*, 396−403.
(47) Tofts, P. S., Brix, G., Buckley, D. L., Evelhoch, J. L., Henderson, E., Knopp, M. V., Larsson, H. B., Lee, T. Y., Mayr, N. A., Parker, G. J., Port, R. E., Taylor, J., and Weisskoff, R. M. (1999) Estimating kinetic parameters from dynamic contrast-enhanced T(1)-weighted MRI of a diffusable tracer: standardized quantities and symbols. *J. Magn. Reson. Imaging 10*, 223−232.
(48) Narisada, H., Aoki, T., Sasaguri, T., Hashimoto, H., Konishi, T., Morita, M., and Korogi, Y. (2006) Correlation between numeric gadolinium-enhanced dynamic MRI ratios and prognostic factors and histologic type of breast carcinoma. *Am. J. .Roentgenol. 187*, 297−306.
(49) Ao, M., Wang, Z., Ran, H., Guo, D., Yu, J., Li, A., Chen, W., Wu, W., and Zheng, Y. (2010) Gd-DTPA-loaded PLGA microbubbles as both ultrasound contrast agent and MRI contrast agent–a feasibility research. *J. Biomed. Mater. Res., Part B 93*, 551−556.
(50) Yang, F., Li, L., Li, Y., Chen, Z., Wu, J., and Gu, N. (2008) Superparamagnetic nanoparticle-inclusion microbubbles for ultrasound contrast agents. *Phys. Med. Biol. 53*, 6129−6141.
(51) Yang, F., Gu, A. Y., Chen, Z. P., Gu, N., and Ji, M. (2008) Multiple emulsion microbubbles for ultrasound imaging. *Mater. Lett. 62*, 121−124.
(52) Cheung, J. S., Chow, A. M., Guo, H., and Wu, E. X. (2009) Microbubbles as a novel contrast agent for brain MRI. *Neuroimage 46*, 658−664.
(53) Alexander, A. L., McCreery, T. T., Barrette, T. R., Gmitro, A. F., and Unger, E. C. (1996) Microbubbles as novel pressure-sensitive MR contrast agents. *Magn. Reson. Med. 35*, 801−806.
(54) Pisani, N. T. E., Galaz, B., Santin, M., Berti, R., Taulier, N., Kurtisovski, E., Lucidarme, O., Ourevitch, M., Doan, B. T., Beloeil, J. C., Gillet, B., Urbach, W., Bridal, S. L., and Fattal, E. (2008) Perfluorooctyl bromide polymeric capsules as dual contrast agents for ultrasonography and magnetic resonance imaging. *Adv. Funct. Mater. 18*, 2963−2971.
(55) Zhu, Q., Conant, E., and Chance, B. (2000) Optical imaging as an adjunct to sonograph in differentiating benign from malignant breast lesions. *J. Biomed. Opt. 5*, 229−236.
(56) Smith, N. B. (2008) Applications of ultrasonic skin permeation in transdermal drug delivery. *Expert Opin. Drug Delivery 5*, 1107−1120.
(57) Bekeredjian, R., Chen, S., Frenkel, P. A., Grayburn, P. A., and Shohet, R. V. (2003) Ultrasound-targeted microbubble destruction can repeatedly direct highly specific plasmid expression to the heart. *Circulation 108*, 1022−1026.
(58) Lindner, J. R. (2004) Microbubbles in medical imaging: current applications and future directions. *Nat. Rev. Drug Discovery 3*, 527−532.
(59) Hernot, S., and Klibanov, A. L. (2008) Microbubbles in ultrasound-triggered drug and gene delivery. *Adv. Drug Delivery Rev. 60*, 1153−1166.

(60) Benson, R. C., and Kues, H. A. (1978) Fluorescence properties of indocyanine green as related to angiography. *Phys. Med. Biol. 23*, 159−163.
(61) Kupriyanov, V. V., Nighswander-Rempel, S., and Xiang, B. (2004) Mapping regional oxygenation and flow in pig hearts in vivo using near-infrared spectroscopic imaging. *J. Mol. Cell Cardiol. 37*, 947−957.
(62) Elsner, A. E., Zhou, Q., Beck, F., Tornambe, P. E., Burns, S. A., Weiter, J. J., and Dreher, A. W. (2001) Detecting AMD with multiply scattered light tomography. *Int. Ophthalmol. 23*, 245−250.
(63) Zheng, X., Zhou, F., Wu, B., Chen, W. R., and Xing, D. (2012) Enhanced Tumor Treatment using biofunctional indocyanine green-containing nanostructure by intratumoral or intravenous injection. *Mol. Pharmaceut. 9*, 514−522.
(64) Kuo, W. S., Chang, C. N., Chang, Y. T., Yang, M. H., Chien, Y. H., Chen, S. J., and Yeh, C. S. (2010) Gold nanorods in photodynamic therapy, as hyperthermia agents, and in near-infrared optical imaging. *Angew. Chem., Int. Ed. 49*, 2711−2715.
(65) Ku, G., and Wang, L. V. (2005) Deeply penetrating photoacoustic tomography in biological tissues enhanced with an optical contrast agent. *Opt. Lett. 30*, 507−509.
(66) Wang, L. V. (2008) Prospects of photoacoustic tomography. *Med. Phys. 35*, 5758−5767.
(67) Rosencwaig, A., and Gersho, A. (1978) Theory of the photoacoustic effect with solids. *J. Appl. Phys. 47*, 64−69.
(68) Song, K. H., Kim, C., Cobley, C. M., Xia, Y., and Wang, L. V. (2009) Near-infrared gold nanocages as a new class of tracers for photoacoustic sentinel lymph node mapping on a rat model. *Nano Lett. 9*, 183−188.
(69) Wang, B., Yantsen, E., Larson, T., Karpiouk, A. B., Sethuraman, S., Su, J. L., Sokolov, K., and Emelianov, S. Y. (2009) Plasmonic intravascular photoacoustic imaging for detection of macrophages in atherosclerotic plaques. *Nano Lett. 9*, 2212−2217.
(70) Li, P. C., Wang, C. R., Shieh, D. B., Wei, C. W., Liao, C. K., Poe, C., Jhan, S., Ding, A. A., and Wu, Y. N. (2008) In vivo photoacoustic molecular imaging with simultaneous multiple selective targeting using antibody-conjugated gold nanorods. *Opt. Express 16*, 18605−18615.
(71) Wilson, K., Homan, K., and Emelianov, S. (2009) Photoacoustic and ultrasound imaging contrast enhancement using a dual contrast agent. *Proc. SPIE 7564*, 75642P.
(72) Wilson, K., Homan, K., and Emelianov, S. (2012) Biomedical photoacoustics beyond thermal expansion using triggered nanodroplet vaporization for contrast-enhanced imaging. *Nat. Commun. 3*, 618.
(73) Kim, C., Qin, R., Xu, J. S., Wang, L. V., and Xu, R. (2010) Multifunctional microbubbles and nanobubbles for photoacoustic and ultrasound imaging. *J. Biomed. Opt. 15*, 010510.
(74) Barnett, B. P., Ruiz-Cabello, J., Hota, P., Ouwerkerk, R., Shamblott, M. J., Lauzon, C., Walczak, P., Gilson, W. D., Chacko, V. P., Kraitchman, D. L., Arepally, A., and Bulte, J. W. (2011) Use of perfluorocarbon nanoparticles for non-invasive multimodal cell tracking of human pancreatic islets. *Contrast Media Mol. Imaging 6*, 251−259.
(75) Barnett, B. P., Arepally, A., Stuber, M., Arifin, D. R., Kraitchman, D. L., and Bulte, J. W. (2011) Synthesis of magnetic resonance-, X-ray- and ultrasound-visible alginate microcapsules for immunoisolation and noninvasive imaging of cellular therapeutics. *Nat. Protoc. 6*, 1142−1151.
(76) Kim, J., Arifin, D. R., Muja, N., Kim, T., Gilad, A. A., Kim, H., Arepally, A., Hyeon, T., and Bulte, J. W. (2011) Multifunctional capsule-in-capsules for immunoprotection and trimodal imaging. *Angew. Chem., Int. Ed. 50*, 2317−2321.
(77) Arifin, D. R., Long, C. M., Gilad, A. A., Alric, C., Roux, S., Tillement, O., Link, T. W., Arepally, A., and Bulte, J. W. (2011) Trimodal gadolinium-gold microcapsules containing pancreatic islet cells restore normoglycemia in diabetic mice and can be tracked by using US, CT, and positive-contrast MR imaging. *Radiology 260*, 790−798.
(78) Ng, K. Y., and Liu, Y. (2002) therapeutic ultrasound: Its application in drug delivery. *Med. Res. Rev. 22*, 204−223.
(79) Hernot, S., and Klibanov, A. L. (2008) Microbubbles in ultrasound-triggered drug and gene delivery. *Adv. Drug Delivery Rev. 60*, 1153−1166.
(80) Unger, E. C., Porter, T., Culp, W., Labell, R., Matsunaga, T., and Zutshi, R. (2004) Therapeutic applications of lipid-coated microbubbles. *Adv. Drug Delivery Rev. 56*, 1291−1314.
(81) Liu, Y. Y., Miyoshi, H., and Nakamura, M. (2006) Encapsulated ultrasound microbubbles: Therapeutic application in drug/gene delivery. *J. Controlled Release 114*, 89−99.
(82) Sirsi, S. R., and Borden, M. A. (2012) Advances in ultrasound mediated gene therapy using microbubble contrast agents. *Theranostics 2*, 1208−1222.
(83) Porter, T. R., and Xie, F. (2001) Ultrasound, microbubbles, and thrombolysis. *Prog. Cardiovasc. Dis. 44*, 101−110.
(84) Petit, B., Yan, F., Tranquart, F., and Allémann, E. (2012) Microbubbles and ultrasound-mediated thrombolysis: a review of recent in vitro studies. *J. Drug Delivery Sci. Technol. 22*, 381−392.
(85) Chen, J., Glaus, C., Laforest, R., Zhang, Q., Yang, M., Gidding, M., Welch, M. J., and Xia, Y. (2010) Gold nanocages as photothermal transducers for cancer treatment. *Small 6*, 811−817.
(86) Hirsch, L. R., Stafford, R. J., Bankson, J. A., Sershen, S. R., Rivera, B., Price, R. E., Hazle, J. D., Halas, N. J., and West, J. L. (2003) Nanoshell-mediated near-infrared thermal therapy of tumors under magnetic resonance guidance. *Proc. Natl. Acad. Sci. U. S. A. 100*, 13549−13554.
(87) Jang, B., Park, J. Y., Tung, C. H., Kim, I. H., and Choi, Y. (2011) Gold nanorod-photosensitizer complex for near-infrared fluorescence imaging and photodynamic/photothermal therapy in vivo. *ACS Nano 5*, 1086−1094.
(88) Choi, W. I., Kim, J. Y., Kang, C., Byeon, C. C., Kim, Y. H., and Tae, G. (2011) Tumor regression in vivo by photothermal therapy based on gold-nanorod-loaded, functional nanocarriers. *ACS Nano 5*, 1995−2003.
(89) Moon, H. K., Lee, S. H., and Choi, H. C. (2009) In vivo near-infrared mediated tumor destruction by photothermal effect of carbon nanotubes. *ACS Nano 3*, 3707−3713.
(90) Zhou, F., Xing, D., Ou, Z., Wu, B., Resasco, D. E., and Chen, W. R. (2009) Cancer photothermal therapy in the near-infrared region by using single-walled carbon nanotubes. *J. Biomed. Opt. 14*, 021009.
(91) Yang, K., Zhang, S., Zhang, G., Sun, X., Lee, S. T., and Liu, Z. (2010) Graphene in mice: ultrahigh in vivo tumor uptake and efficient photothermal therapy. *Nano Lett. 10*, 3318−3323.
(92) Burke, A., Ding, X., Singh, R., Kraft, R. A., Levi-Polyachenko, N., Rylander, M. N., Szot, C., Buchanan, C., Whitney, J., Fisher, J., Hatcher, H. C., D'Agostino, R., Jr., Kock, N. D., Ajayan, P. M., Carroll, D. L., Akman, S., Torti, F. M., and Torti, S. V. (2009) Long-term survival following a single treatment of kidney tumors with multiwalled carbon nanotubes and near-infrared radiation. *Proc. Natl. Acad. Sci. U. S. A. 106*, 12897−12902.
(93) Zhang, M., Murakami, T., Ajima, K., Tsuchida, K., Sandanayaka, A. S., Ito, O., Iijima, S., and Yudasaka, M. (2008) Fabrication of ZnPc/protein nanohorns for double photodynamic and hyperthermic cancer phototherapy. *Proc. Natl. Acad. Sci. U. S. A. 105*, 14773−14778.
(94) Li, Y., Lu, W., Huang, Q., Huang, M., Li, C., and Chen, W. (2010) Copper sulfide nanoparticles for photothermal ablation of tumor cells. *Nanomedicine 5*, 1161−1171.
(95) Fu, G. L., Liu, W., Feng, S. S., and Yue, X. L. (2012) Prussian blue nanoparticles operate as a new generation of photothermal ablation agents for cancer therapy. *Chem. Commun. 48*, 11567−11569.
(96) Zha, Z. B., Yue, X. L., Ren, Q. S., and Dai, Z. F. (2013) Uniform polypyrrole nanoparticles with high photothermal conversion efficiency for photothermal ablation of cancer cells. *Adv. Mater. 25*, 777−782.
(97) Ke, H. T., Wang, J. R., Dai, Z. F., Jin, Y. S., Qu, E. Z., Xing, Z. W., Guo, C. X., Yue, X. L., and Liu, J. B. (2011) Gold-nanoshelled microcapsules: a theranostic agent for ultrasound contrast imaging and photothermal therapy. *Angew. Chem., Int. Ed. 50*, 3017−3021.
(98) Ke, H. T., Wang, J. R., Tong, S., Jin, Y. S., Wang, S. M., Qu, E. Z., Bao, G., and Dai, Z. F. (2014) Gold nanoshelled liquid

perfluorocarbon magnetic nanocapsules: a nanotheranostic platform for bimodal ultrasound/magnetic resonance imaging guided photothermal tumor ablation. *Theranostics 4*, 12−23.
(99) Ke, H. T., Yue, X. L., Jin, Y. S., Xing, S., Zhang, Q., Dai, Z. F., Tian, J., Wang, S. M., and Jin, Y. S. (2014) Gold nanoshelled liquid perfluorocarbon nanocapsules for combined dual modal ultrasound/CT imaging and photothermal therapy of cancer. *Small 10*, 1220−1227.
(100) Li, Y. B., Lu, W., Huang, Q. A., Huang, M. A., Li, C., and Chen, W. (2010) Copper sulfide nanoparticles for photothermal ablation of tumor cells. *Nanomedicine 5*, 1161−1171.
(101) Zha, Z. B., Wang, S. M., Zhang, S. H., Qu, E. Z., Ke, H. T., Wang, J. R., and Dai, Z. F. (2013) Targeted delivery of CuS nanoparticles through ultrasound image-guided microbubble destruction for efficient photothermal therapy. *Nanoscale 5*, 3216−3219.
(102) Zhang, G. D., Yang, Z., Lu, W., Zhang, R., Huang, Q., Tian, M., Li, L., Liang, D., and Li, C. (2009) Influence of anchoring ligands and particle size on the colloidal stability and in vivo biodistribution of polyethylene glycol-coated gold nanoparticles in tumor-xenografted mice. *Biomaterials 30*, 1928−1936.
(103) Burns, A. A., Vider, J., Ow, H., Herz, E., Penate-Medina, O., Baumgart, M., Larson, S. M., Wiesner, U., and Bradbury, M. (2009) Fluorescent silica nanoparticles with efficient urinary excretion for nanomedicine. *Nano Lett. 9*, 442−448.
(104) Yang, J., Choi, J., Bang, D., Kim, E., Lim, E. K., Park, H., Suh, J. S., Lee, K., Yoo, K. H., Kim, E. K., Huh, Y. M., and Haam, S. (2011) Convertible organic nanoparticles for near-infrared photothermal ablation of cancer cells. *Angew. Chem., Int. Ed. 50*, 441−444.
(105) Cheng, L., Yang, K., Chen, Q., and Liu, Z. (2012) Organic stealth nanoparticles for highly effective in vivo near-infrared photothermal therapy of cancer. *ACS Nano 6*, 5605−5613.
(106) Kai, Y., Xu, H., Cheng, L., Sun, C. Y., Wang, J., and Liu, Z. (2012) In vitro and in vivo near-infrared photothermal therapy of cancer using polypyrrole organic nanoparticles. *Adv. Mater. 24*, 5586−5592.
(107) Chen, M., Fang, X. L., Tang, S. H., and Zheng, N. F. (2012) Polypyrrole nanoparticles for high-performance in vivo near-infrared photothermal cancer therapy. *Chem. Commun. 48*, 8934−8936.
(108) Zha, Z. B., Wang, J. R., Qu, E. Z., Zhang, S. H., Jin, Y. S., Wang, S. M., and Dai, Z. F. (2003) Polypyrrole hollow microspheres as echogenic photothermal agent for ultrasound imaging guided tumor ablation. *Sci. Rep. 3*, 2360.
(109) Zha, Z. B., Wang, J. S., Zhang, S. H., Wang, S. M., Qu, E. Z., Zhang, Y. Y., and Dai, Z. F. (2014) Engineering of perfluorooctylbromide polypyrrole nano-/microcapsules for simultaneous contrast enhanced ultrasound imaging and photothermal treatment of cancer. *Biomaterials 35*, 287−293.
(110) Zha, Z. B., Deng, Z. J., Li, Y. Y., Li, C. H., Wang, J. R., Wang, S. M., Qu, E. Z., and Dai, Z. F. (2013) Biocompatible polypyrrole nanoparticles as a novel organic photoacoustic contrast agent for deep tissue imaging. *Nanoscale 5*, 4462−4467.
(111) Jin, Y. S., Wang, J. R., Ke, H. T., Wang, S. M., and Dai, Z. F. (2013) Graphene oxide modified PLA microcapsules containing gold nanoparticles for ultrasonic/CT bimodal imaging guided photothermal tumor therapy. *Biomaterials 34*, 4794−4802.
(112) Li, X. D., Liang, X. L., Yue, X. L., Wang, J. R., Li, C. H., Deng, Z. J., Jing, L. J., Lin, L., Qu, E. Z., Wang, S. M., Wu, C. L., Wu, H. X., and Dai, Z. F. (2014) Imaging guided photothermal therapy using iron oxide loaded poly(lactic acid) microcapsules coated with graphene oxide. *J. Mater. Chem. B 2*, 217−223.
(113) Nahrendorf, M., and Sosnovik, D. E. (2011) Science to practice: will magnetic guidance of microbubbles play a role in clinical molecular imaging? *Radiology 260*, 309−310.